

Prediction of the deflagration index for organic dusts as a function of the mean particle diameter

Anna Fumagalli ^a, Marco Derudi ^a, Renato Rota ^a, Jef Snoeys ^b, Sabrina Copelli ^{c,*}

^a Politecnico di Milano, Dipartimento di Chimica, Materiali e Ingegneria Chimica, "G. Natta", via Mancinelli 7, 20131, Milano, Italy

^b Fike Corporation, 704 SW 10th Street, Blue Springs, MO, United States

^c Università degli Studi dell'Insubria, Dipartimento di Scienza e Alta Tecnologia, via G.B. Vico 46, 21100, Varese, Italy

All the recently occurred accidents involving powdered materials demonstrate that dust explosion is up to now an open problem. To mitigate the effects of this phenomenon on people, environment and equipment, it is important to understand the characteristics of the potentially explosive material which can affect the violence of a dust explosion. The deflagration index is the most relevant recognized parameter able to measure the severity of such a phenomenon. Among all the critical issues affecting the use of this parameter for industrial safety, the particle size distribution of the tested powder plays a relevant role. In this paper, a simple but reliable mathematical model has been proposed to describe the effect of the mean particle diameter on the dust explosibility. Model predictions have been compared with both literature and new experimental data in order to validate the general proposed approach.

Keywords:

Dust explosion

Deflagration index

Explosion severity

Modeling Experimental

K_{St} data

1. Introduction

At present, both gas and dust explosions are a "credible risk" because they continue to both destroy industries and kill or injure workers (NFPA, 2015; Casson Moreno and Cozzani, 2015).

Considering that the first dust explosion extensively investigated in Europe occurred in 1785, at the Mr. Giacomelli's bakery in Turin (Eckhoff, 2003), it is not surprising that the history of process safety is marked by several dust explosions; some of these accidents have been seared into the people consciousness and have helped to build up the basis of the industrial safety. For this reason, during the last years, the dust explosion phenomenon has been extensively investigated and different mitigation techniques have been developed (Eckhoff, 2003). However, several severe accidents still keep on recurring (CBS, 2017; DUST_EXPLOSION_RESEARCH, 2017), such as: 1) the violent polyethylene dust explosion occurred at the "West Pharmaceutical Services" in Kinston, North Carolina (2003); 2) the devastating sugar powder explosion which took place at the "Imperial Sugar Company" in Port Wentworth (2008); 3) the incident occurred at the "Zhongrong Metal Production Company", an automotive parts factory located in Kunshan

(2014), where a strong metal powder explosion killed 146 workers; 4) the flammable starch-based powder explosion which happened at the "Formosa Fun Coast" in New Taipei (2015) and injured 508 people; and, finally, 5) the recent flour mill explosion, occurred in the United Kingdom (2015), where 4 workers were killed.

In order to both prevent and protect people and plants from these types of accident, it is fundamental to characterize the hazard related to each powder. Since the deflagration index (K_{St}) is capable of representing in a single value the expected violence of a dust explosion, it is widely used as a key parameter in the vent sizing of industrial equipment (NFPA, 2013). Such a parameter depends on the type of dust as well as on its humidity content and particle size distribution. Particularly, considering the particle size distribution, it is quite common finding different mean diameters in distinct areas of the same plant. This happens, for instance, when using granulating and milling processes in pharmaceutical and food industries. Knowing that the value of K_{St} is strongly affected by the mean dust diameter (Eckhoff, 2003), the deflagration index should be evaluated for each characteristic dimension, to estimate the hazard related to the manufacturing of a certain dust. Even if the K_{St} value is usually measured using a 20 L apparatus (ASTM, 2012) instead of the standard 1 m³ one, a significant amount of resources (in terms of both amount of material and time spent for the analysis) are unavoidably required for a complete characterization of

* Corresponding author.

E-mail address: sabrina.copelli@uninsubria.it (S. Copelli).

the hazard associated to a certain powder in different plant areas. This occurs because of the fact that a single K_{St} value, for a given mean particle diameter, is calculated through an experimental procedure that consists of several “explosion tests” at different dust concentrations inside the apparatus: this is done in order to detect the maximum of a series of K_{St} values, that is the characteristic K_{St} for a given powder.

Consequently, in the last years, some mathematical models have been proposed to predict the deflagration index values (see Fumagalli et al., 2016 for a brief review of such models). If a reliable mathematical model would be available, it could be used to significantly reduce the amount of resources required in the hazard assessment procedure. In particular, this would be relevant for Small and Medium Enterprises (SMEs) which cannot allocate too large amount of resources when changing the typology of processed dust.

Therefore, the main aim of this work is to develop a simple but reliable mathematical model able to predict the value of the deflagration index for an organic powder when its mean particle size changed in a quite wide range of characteristic dimensions. Within this frame, a series of innovative approaches has been implemented. First of all, a single experimental value of K_{St} has been coupled with the results coming from the proposed model to estimate the dependency of the deflagration index on the mean particle diameter variation: this permits to avoid the experimental characterizations in correspondence of each mean particle size of the analyzed dust but it also guarantees a reliable estimation of the powder K_{St} since an experimental value at a given mean diameter is used. Then, the material balance on the solid phase has been written considering only the reactive portion of the dust particle (the non-reactive solid residue has been properly taken into account by measuring its value through a standard thermogravimetric test). Moreover, the ensemble of “quasi-spherical” dust particles which face the flame front during the explosion has been sketched as an equivalent slab of indefinite length, which possesses a thickness equal to the mean diameter of the dust particle. Finally, the characteristic length of a single powder particle (that is, the thickness of the equivalent slab facing the flame front) has been considered constant during the explosive phenomenon: this implies that the porosity of the dust increases during time.

To assess the reliability of the proposed approach a few experiments have been carried out in the standard 20 L apparatus to measure the K_{St} values at different mean particle diameter. These data, together with other data from the literature, have been compared with the model predictions showing a good agreement, therefore confirming the reliability of the proposed approach.

2. Mathematical model

For organic dust clouds, pyrolysis/devolatilization followed by gas-phase combustion of the pyrolysis gases (also called “volatiles”) has been proposed as the dominant mechanism through which a combustible dust explodes (Hertzberg et al., 1988; Cashdollar et al., 1989; Eckhoff, 2003). In particular, Di Benedetto et al. (2010) developed a single particle model able to predict the variation of the deflagration index as a function of the mean diameter for organic powders based on the following assumptions: 1) evaluation of the volatiles production rate through a pyrolysis kinetic model and 2) evaluation of K_{St} as a function of the volatiles production rate. Along the same lines, a new simple but reliable mathematical model has been developed and validated, as discussed in the following sections. The aim of such a new model is not to provide a fully “a priori” prediction of the K_{St} value (which is a very challenging task considering the high complexity of all the physico-chemical phenomenon in a dust explosion), but a simple tool to

extrapolate a K_{St} value measured for a given dust mean diameter (particularly, a value lower than 50 μm , if possible) to other diameter values (anyway under 500 μm , which is considered the threshold value beyond which a powder can be considered non-explosive).

It should be noted that the choice of using the mean dust diameter instead of other parameters that correlate better with explosion severity (such as the Sauter mean diameter, the BET specific surface area, or the polydispersity) is justified by the main aim of this work, that is, the development of a simple mathematical model able to predict the variation of the K_{St} with the particle size through a minimum experimental efforts. Moreover, as the larger part of the data used to validate the model developed in this work have been taken from the literature, where neither particle surface areas nor particle size distribution have been reported, such parameters could not be calculated.

2.1. Model assumptions

In order to describe the violence of an organic dust explosion (that is, the K_{St} value), an approach based on the description of the pyrolysis/devolatilization kinetics can be used. The unknown kinetic parameters of the pyrolysis/devolatilization process for a given dust can be estimated by fitting of thermogravimetric (TG) data, which describe the extent of dust decomposition as a function of temperature. This approach is not only quite fast and simple, but it also exploits the advantage of characterizing the mass loss (that is the devolatilization/pyrolysis process) through a kinetic equation as a function of both the temperature and the residual solid mass.

However, it should be mentioned that in a real dust explosion the devolatilization/pyrolysis reaction is a very complex and fast process, whose characteristics can be better investigated using pyrolysis-GC-MS measurements. Such data should be used as far as they are available.

The processes involved in the volatiles production from the solid particle can be described through a suitable system of partial differential equations, representing both material (for solid phase and volatiles) and energy balances on a single particle of dust under the following assumptions:

- 1) in the 20 L Siwek sphere (Siwek, 1977), used for the K_{St} measurement, a flame front, generated by the combustion of volatiles previously released by other burning particles, moves towards the unburned particles;
- 2) the combustion of volatiles is instantaneous (in other words, the gas phase combustion characteristic time never controls the dynamics of the process, at least for what concerns the determination of the K_{St} value); this assumption implies the existence of a critical mean diameter for the validity of the mathematical model since above 100–150 μm discrete diffusion flames can occur;
- 3) the system is one-dimensional in space (described in Cartesian coordinates); in fact, the ensemble of pseudo-spherical particles facing the temperature flame front can be considered equivalent to a slab of indefinite length, whose thickness is equal to the mean diameter of a dust particle; such a slab contacts the high temperature flame front only on one side, as sketched in Fig. 1. This schematization of the particle heating and pyrolysis phenomena is one of the novelty of this work which permits to notably simplify the equations describing the overall explosive process;
- 4) negligible resistance to mass transfer and negligible diffusive flux with respect to the convective one for the volatiles (pyrolysis products) leaving the particle in the gas phase;
- 5) no secondary reactions of volatiles, apart from their combustion, after they leave the particle;

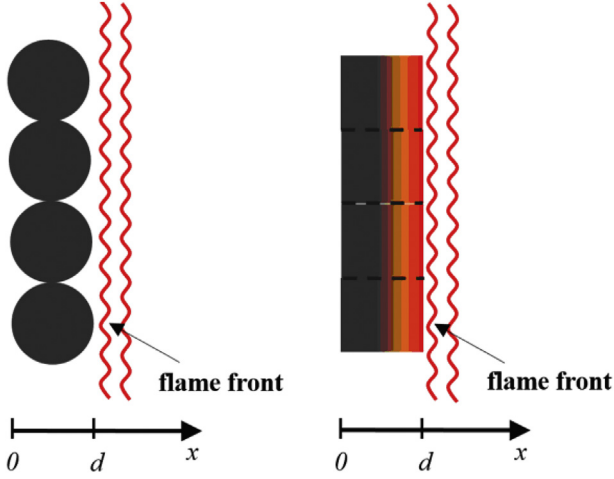


Fig. 1. Mono-dimensional model for the particle heating and pyrolysis.

- 6) local thermal equilibrium between solid and volatiles;
- 7) pseudo-steady-state for the gas phase comprised into the particle volume, which means that no volatiles are accumulated inside the dust particle;
- 8) particles with constant volume; that is, when a solid particle is consumed by the pyrolysis reaction, a solid skeleton of pyrolyzed substance is generated, increasing the particle porosity during the devolatilization process; this also means that not all the particle mass is consumed since some residual can be found at the end of the pyrolysis process. This approach is substantially different with respect to that one used in previous models (Di Benedetto et al., 2010) where a classical shrinking core model has been considered;
- 9) molar and mass specific velocities are considered equal;
- 10) the convective heat transfer coefficient between gas and solid particle (h_c) can be evaluated through standard correlations developed for turbulent conditions, which are typical of a 20 L sphere experiment (Pu et al., 1990; Zhen and Leuckel, 1996; Dahoe et al., 2001, 2002);
- 11) in the energy balance equation, variations of the apparent solid density are taken into account by considering a mean effective solid density (that is, a constant mean porosity) which is assumed constant for all the process duration (this is done in order to solve the system of PDEs).

2.2. Model equations

Pyrolysis of the solid particle (S) has been described by the following global reaction:



leading to the pyrolysis products (volatiles), P .

Using the aforementioned hypotheses as well as this devolatilization kinetic model, material and energy balance equations lead to the equations summarized in the following. Particularly, the material balance equation on the solid phase may be written as:

$$\frac{\partial \bar{\rho}_S}{\partial t} = -r \quad (2)$$

where $\bar{\rho}_S$ is the reacting density of the dust particle (that is the ratio of the dust particle reacting mass with respect to its initial volume,

V_0) and $r = k \cdot \bar{\rho}_S^n$ is the single-step devolatilization reaction rate. It is important to note that $\bar{\rho}_S$ in Eq. (2) is a function of both time and space since the reaction rate depends on the temperature inside the slab (which will be described by a PDE).

According to the aforementioned assumptions, the particle is consumed increasing its porosity and leaving a skeleton with the same initial volume; this means that only a part of the particle mass is consumed by the pyrolysis/devolatilization process. The mass that can be consumed will be referred in the following as the “reacting mass” of the particle. Hence, at the initial time the reacting mass is as $m_{S,0} = m_{S,0} - m_{S,0} \cdot \beta$, where $m_{S,0}$ is the total initial particle mass, and β is the fraction of such a mass that is not consumed by the pyrolysis/devolatilization process leading to the particle skeleton. Therefore, β is defined as the ratio between the residual mass found at the end of the pyrolysis/devolatilization process ($m_{S,end}$) and the total initial mass ($m_{S,0}$). Accordingly, the initial reacting density of the particle is $\bar{\rho}_{S,0} = m_{S,0} \cdot (1 - \beta) / V_0 = \rho_{S,0} \cdot (1 - \beta)$.

This approach is another innovation with respect to other models proposed in the literature since it permits to take into account the presence of a solid residue without complicating, sometimes without a clear physical justification, the expression of the volatilization reaction rate. The material balance equation on the volatiles/gas phase may be written as:

$$\frac{\partial(\varepsilon \cdot \rho_G)}{\partial t} = r - \frac{\partial(\varepsilon \cdot \rho_G \cdot U_x)}{\partial x} = r - \frac{\partial(v)}{\partial x} \approx 0 \quad (3)$$

where the time derivative has been superimposed equal to zero thanks to the aforementioned pseudo-steady state hypothesis (see hypothesis 7) and v represents the flux of volatiles leaving the particle surface, according to Eq. (4):

$$v = \rho_G \cdot \varepsilon \cdot U_x \quad (4)$$

where ρ_G is the ratio of the mass of volatiles with respect to the particle volume, ε is the particle porosity and U_x is the outward velocity of the volatiles.

Despite this simplification, Eq. (3) still remain a PDE and, consequently, v is a function of both space and time, since the expression of the volatiles production rate contains the temperature inside the slab.

Finally, the energy balance equation on the solid phase may be written under the following main hypothesis:

- heat capacity of the solid phase (S) constant and much greater than that one of the volatiles (P);
- for what concerns the computation of the system enthalpy per unit of volume, we refer only to the gaseous phase (volatiles) because the solid phase can not be subjected to convective fluxes.

$$\rho_{S,eff} \cdot c_{p,S} \cdot \frac{\partial T}{\partial t} = \bar{\lambda} \cdot \frac{\partial^2 T}{\partial x^2} - c_{p,V} \cdot v \cdot \frac{\partial(v \cdot T)}{\partial x} - \Delta H_{rxn} \cdot r \quad (5)$$

where $\rho_{S,eff} = \rho_{S,0} \cdot (1 - \bar{\varepsilon})$ is an effective solid density (see hypothesis 11); $\bar{\varepsilon}$ is a mean porosity (whose value has been considered equal to 0.5); $\bar{\lambda} = \lambda \cdot (1 - \bar{\varepsilon})$ is the effective thermal conductivity; $c_{p,S}$ and $c_{p,V}$ are, respectively, the specific heat of solid and volatiles (which are considered constant since their variations with temperature can be neglected in the range here taken into account) and ΔH_{rxn} is the reaction enthalpy of the pyrolysis/devolatilization process (constant).

It is possible to observe that the new simplifications introduced in Eq. (5) permit an easy solution of the resulting PDE system,

without penalizing the accuracy of the obtained solutions.

As said before, equations (2), (3) and (5) represent a system of three partial differential equations in the three unknown ρ_S , ν and T . In order to solve such a system both boundary and initial conditions must be specified. Particularly, boundary conditions are required for Equation (3) (only one side) and (5) (both sides); initial conditions are required for all the variables but ν .

Boundary Conditions:

$$x = 0 \rightarrow \nu = 0 \quad (6a)$$

$$x = 0 \rightarrow \frac{\lambda}{\rho_{S,0} \cdot c_{p,S}} \frac{\partial T}{\partial x} = 0 \quad (6b)$$

$$x = d \rightarrow \frac{\lambda}{\rho_{S,0} \cdot c_{p,S}} \frac{\partial T}{\partial x} = -\frac{h_c \cdot (T - T_{ext})}{\rho_{S,0} \cdot c_{p,S} \cdot (1 - \bar{\epsilon})} - \frac{e \cdot \sigma \cdot (T^4 - T_{ext}^4)}{\rho_{S,0} \cdot c_{p,S} \cdot (1 - \bar{\epsilon})} \quad (6c)$$

Initial conditions:

$$\begin{cases} \bar{\rho}_S = \rho_{S,0} \cdot (1 - \beta) \\ T = T_0 \end{cases} \quad (6d)$$

where d is the mean particle diameter (m), h_c is the heat transfer coefficient ($\text{W m}^{-2} \text{K}^{-1}$) (computed as reported in Çengel, 2008), T_{ext} is the external flame temperature (K), T_0 is the initial particle temperature, considered equal to 300 (K), e is the emissivity (–) and σ is the Stefan–Boltzmann constant ($\text{W m}^{-2} \text{K}^{-4}$). It is worth to notice that the initial condition for Eq. (2) (first I.C. in Eq. (6d)) contains the piece of information related to the solid residue which is unavoidably found after the explosive process.

Solving such a system of partial differential equations is not a trivial task; in the following section, a simple and robust numerical algorithm specifically modified for this work is briefly presented.

2.3. Numerical algorithm

The system constituted by Equations (2), (3) and (5) has been numerically solved using the Method Of Lines (MOL) (Schiesser, 1991) with the spatial derivatives approximated using various finite differences schemes (Vande Wouwer et al., 2014) which are computed using suitable differentiation matrixes evaluated with the procedure proposed by Fornberg (1988, 1998). This leads to a system of Differential Algebraic Equations (DAEs), which is a general case of system of ordinary differential equations (ODEs) for vector-valued functions in one independent variable. A DAEs system is not directly solvable because, for some derivatives, the time dependence does not appear explicitly. The main distinction between an ODEs and a DAEs system is that the Jacobian matrix is singular for the last system (Ascher and Petzold, 1998); therefore DAEs are generally more difficult to solve numerically with respect to simple ODEs (Ilchmann and Reis, 2014). Therefore, time integration of the resulting semi-discrete ODEs has been carried out through the MATLAB® ode15s function, together with a mass matrix that is used to set the temporal derivatives of the volatiles material balance equation equal to zero, solving in this way the corresponding algebraic equation. According the authors' knowledge, such a simple but effective trick to handle the criticality represented by Eq. (3) has not be previously used to solve system of this type with the MOLs. Particularly, the resulting algorithm has been found to be robust and efficient; providing a fast and reliable solutions. A simple constant step has been used for the finite differences approximation with a five-point centered scheme (for both the first and second spatial derivatives). It has been verified

that both a non-constant step for spatial derivatives and different finite differences schemes (either centered or upward) did not improve neither the reliability nor the precision of the solution. The same observations can be done even increasing the number of discretization points from 300 to 1000: the solution remains the same.

For the sake of example, a typical heating history of a small particle computed through the proposed mathematical model is shown in Fig. 2.

2.4. K_{St} prediction as a function of the mean diameter

The prediction of the deflagration index K_{St} for a given dust mean diameters has been carried out along the lines proposed by Di Benedetto et al. (2010) (even if other approaches have been presented in the literature, as that one of Reyes et al., 2011), that is, by matching the ratio of the maximum production rates of the volatile leaving the particle ($VPR(d) = \max(\nu(x = d, t))$) at two different dust mean diameters to the ratio of the corresponding K_{St} values:

$$K_{St}(d) = \frac{VPR(d)}{VPR(d_{exp})} \cdot K_{St}(d_{exp}) \quad (7)$$

The main difference with respect to the previously proposed approach is that, here d_{exp} is a reference mean diameter, possibly but not necessarily under 50 μm , for which the corresponding $K_{St}(d_{exp})$ value has to be measured through experiments in the 20 L sphere. It should be noted that the reference diameter d_{exp} is not necessarily the limiting particle size below which the K_{St} value does not increase anymore, as required by the approach proposed by Di Benedetto et al. (2010). In this work, the experimental value $K_{St}(d_{exp})$ is simply a reference value, possibly but not necessarily related to the limiting particle size. The use of such a reference experimental K_{St} value is a key feature of the proposed developed model since it recovers in an effective way the main approximations introduced in the model that do not change significantly when changing the particle size (for instance, local high concentrations and agglomerations generated by the velocity difference which exists between the surrounding gases and suspended particles).

As another difference with respect to the approach of Di Benedetto et al. (2010) the values of $\nu(x = d, t)$ and $\nu(x = d_{exp}, t)$ can be directly evaluated by solving the PDE system expressed by

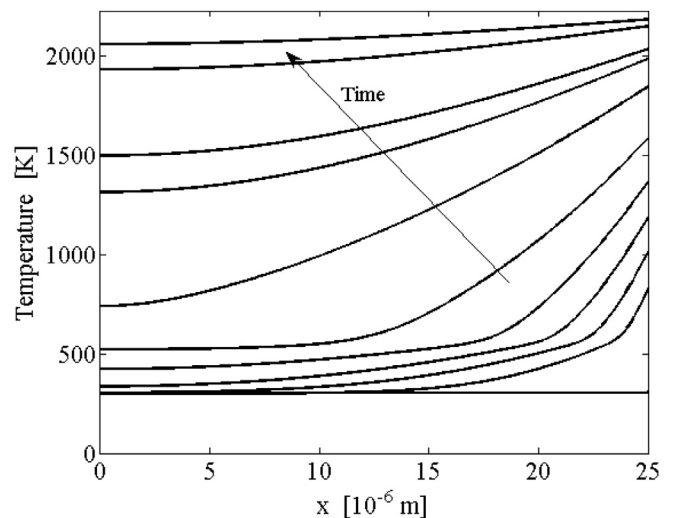


Fig. 2. Temperature distribution inside a sugar particle at different times.

Equations (2), (3) and (5) for the particle diameters equal to d and d_{exp} , respectively (this means that no further calculations are required in order to compute the rate at which the volatiles leave the particle, which is the reference parameter that it has been directly associated with the violence of an organic dust explosion).

3. Results and discussion

The effect of the particle size on the dust explosion parameters has been extensively analyzed during the last years by different researchers (Eckhoff, 2003, 2009; Abbasi and Abbasi, 2007). Hence, it is well known that the deflagration index decreases when the mean particle diameter increases. However, the literature data available at different dust mean diameters are not always carried out under the same conditions (humidity, ignition delay time, nozzle type, cooling mode, degree of cleaning of the sphere wall, and so on), making difficult to understand clearly the K_{St} vs. diameter trends. In order to validate the proposed model, some literature data have been used concerning polyethylene (Di Benedetto et al., 2010) and sugar (GESTIS-DUST-EX, 2016), whose K_{St} vs. diameter experimental values have been summarized in Fig. 3.

In addition, the same figure reports also some new experimental results obtained for niacin (using a standard 20 L Siwek apparatus located in the Fike Europe's Laboratories at Herentals, Belgium), which is the dust used for the Calibration-Round-Robin competition, following the ASTM-E1226 standard (ASTM, 2012). The advantages of niacin are the general low moisture content, which minimizes the tendency to an inter-particle aggregation, and a relative small particle size, which guarantees a fast combustion with a small amount of unburned residues.

We can see, from the data summarized in Fig. 3, that the K_{St} value always decreases as the dust mean diameter increases; the measured values of the K_{St} for the three dusts are in a range from about 0 up to 300 (bar m s^{-1}). For all the dusts investigated, the smallest diameter value has been selected as the reference value, d_{exp} . Moreover, the mathematical model previously discussed involves some other constitutive parameters. For what concerns the physical parameters, the values reported in Table 1 have been used. The kinetic parameters of the single-reaction mechanism (see Eq. (1)) have been estimated by fitting experimental data measured through thermogravimetric analysis (TG). For sugar and niacin TG

experimental trends have been measured in this work, while for polyethylene the TG data have been taken from literature (Contat-Rodrigo et al., 2002).

A modified Arrhenius equation has been used to fit the TG results:

$$k = A \cdot e^{\left(\frac{E \cdot (1 - \chi \cdot \alpha)}{R \cdot T} \right)} \quad (8)$$

where R is the universal gas constant, T is the temperature, α is the TG calorimetric conversion evaluated from the mass loss, A is the pre-exponential factor, E is the activation energy and χ is a correction factor which has the global effect of modifying the value of the activation energy, so making the exponential term depending on both temperature and the solid conversion. Such an expression accounts, in an effective way, for the solid composition change that unavoidably occurred during the pyrolysis/devolatilization process and allows for describing the pyrolysis kinetics using a simple lumped reaction.

All the TG analyses of sugar, niacin and polyethylene shown a solid residue at the end of the test. In order to account for only the reacting solid that contributes to the pyrolysis/devolatilization process, the solid mass (m_S) vs temperature (T) data measured by the TG experiments have been processed by subtracting a quantity equal to $m_{S,0} \cdot \beta$, therefore generating a new variable $\overline{m}_S(T) = m_S(T) - m_{S,0} \cdot \beta$, which starts from $\overline{m}_{S,0} = m_{S,0} \cdot (1 - \beta)$ and ends up in $\overline{m}_{S,end} = m_{S,0} \cdot \beta - m_{S,0} \cdot \beta = 0$.

Following this scheme, the conversion of the reacting solid to the volatiles species is always complete and it is defined as:

$$\alpha = \frac{\overline{m}_{S,0} - \overline{m}_S}{\overline{m}_{S,0}} = \frac{\rho_{S,0} \cdot (1 - \beta) - \overline{\rho}_S}{\rho_{S,0} \cdot (1 - \beta)} \quad (9)$$

As previously discussed, $\overline{\rho}_S = \overline{m}_S / V_0$, where V_0 is the total particle volume.

From the mass balance equation (2) we can easily deduce the following equation:

Table 1
Property of the investigated dusts.

Dust	Parameter	Value	References
Polyethylene	$\rho_{S,0}$ [kg/m^3]	920	Rabinovitch, 1965
	c_p [$\text{J}/(\text{kg} \cdot \text{K})$]	2300	Staggs, 2000
	λ [$\text{W}/(\text{m} \cdot \text{K})$]	0.5	Piergiovanni and Limbo, 2010
	c_v [$\text{J}/(\text{kg} \cdot \text{K})$]	2500	Di Blasi, 1997
	e [-]	0.920	Maestre-Valero et al., 2011
	β [-]	0.018	Contat-Rodrigo et al., 2002
	T_{ext} [K]	2370	Glassman and Yetter, 2008
Sugar	$\rho_{S,0}$ [kg/m^3]	1590	ICSC, 2003
	c_p [$\text{J}/(\text{kg} \cdot \text{K})$]	1263	Anderson et al., 1950
	λ [$\text{W}/(\text{m} \cdot \text{K})$]	0.167	Maccarthy and Fabre, 1989
	c_v [$\text{J}/(\text{kg} \cdot \text{K})$]	2125	Halford, 1957
	e [-]	0.950	Sobrinho et al., 2002
	β [-]	0.207	This work
	T_{ext} [K]	2226	Glassman and Yetter, 2008
Niacin	$\rho_{S,0}$ [kg/m^3]	1162	Agreda, 2007
	c_p [$\text{J}/(\text{kg} \cdot \text{K})$]	1243	Agreda, 2007
	λ [$\text{W}/(\text{m} \cdot \text{K})$]	1.0	Agreda, 2007
	c_v [$\text{J}/(\text{kg} \cdot \text{K})$]	2125	Halford, 1957
	e [-]	0.920	-
	β [-]	0.002	This work
	T_{ext} [K]	2226	Glassman and Yetter, 2008

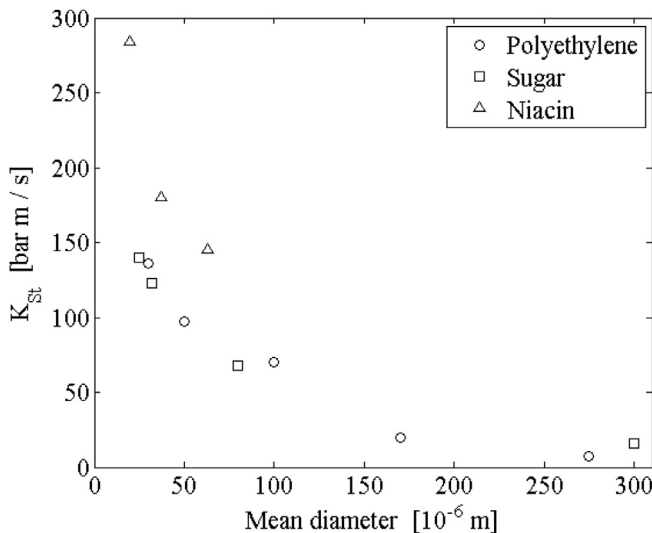


Fig. 3. Experimental K_{St} values for different mean dust diameters.

Table 2
Kinetic parameter values estimated from TG measurements and reaction enthalpy values.

Dust	Parameter	Value	References
Sugar	A	8.41×10^{19}	This work
	E [J/mol]	4.06×10^5	This work
	n	8.02	This work
	x	-0.09	This work
	ΔH [J/kg]	8.00×10^5	Mohos, 2010
Niacin	A	1.97×10^{18}	This work
	E [J/mol]	1.73×10^5	This work
	n	1.00	This work
	x	0.02	This work
	ΔH [J/kg]	2.02×10^5	CHETAH, 2009
Polyethylene	A	9.37×10^{14}	This work
	E [J/mol]	2.02×10^5	This work
	n	0.99	This work
	x	0.10	This work
	ΔH [J/kg]	9.60×10^5	Wichman, 1986

$$\frac{d\alpha}{dt} = A \cdot e^{\left(\frac{-E \cdot (1-x-\alpha)}{R \cdot T}\right)} \cdot [\rho_{S,0}(1-\beta)]^{n-1} \cdot (1-\alpha)^n \quad (10)$$

The estimated kinetic parameters values for sugar, niacin and polyethylene are summarized in Table 2, while the TG measurements together with the fitting results are summarized in Figs. 4–6 in terms of reacting solid conversion vs. temperature.

It is important to stress that A , E , n and x are fitting parameters, whose values have been determined through a suitable minimization of an objective function defined by the summation of the squares differences between experimental and theoretical mass losses vs. temperature.

These kinetic parameters, together with the data summarized in Table 1, have been used to predict the $VPR(d)$ values for the three dusts considered in this work. The flame temperature and the volatile heat capacities of sugar and niacin have been referred to methane since it has been found to be the major compound contributing to the gas phase combustion (Wang et al., 2014; CHETAH, 2009). However, for polyethylene the flame temperature has been referred to ethylene, which is the main volatile product

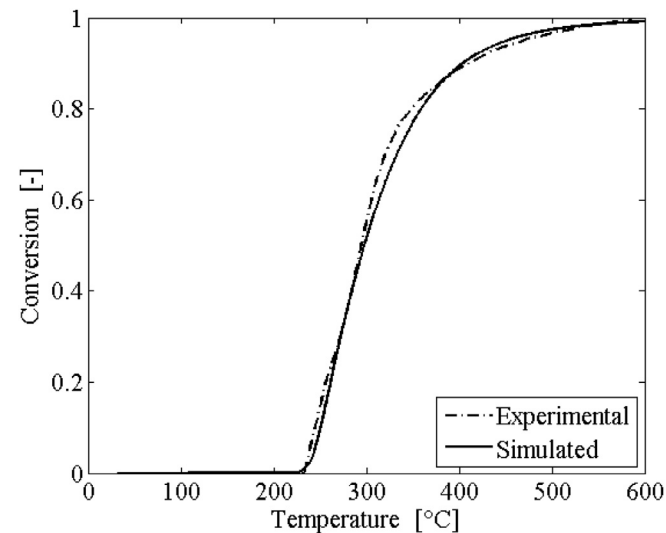


Fig. 4. Experimental and fitted conversion vs. temperature data for sugar. TG measurements carried out at 10 °C/min heating rate.

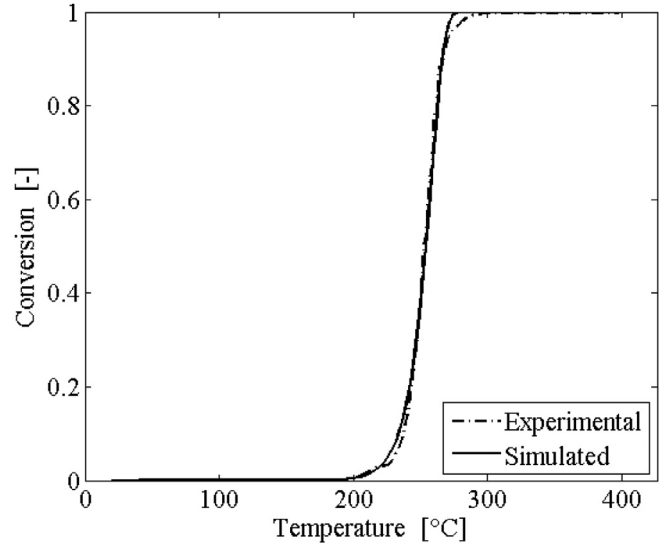


Fig. 5. Experimental and fitted conversion vs. temperature data for niacin. TG measurements carried out at 10 °C/min heating rate.

(Di Benedetto and Russo, 2007). No literature data are available for the emissivity of niacin; therefore the emissivity value for polyethylene has been used. A sensitivity analysis verified that the model results are not strongly sensitive to this parameter.

The system of Equations (2), (3) and (5) has been implemented in a MATLAB® code using a 500 points spatial grid and a global integration time of 100 ms. As expected, the volatile production rate as a function of time shows a maximum, as summarized for the sake of example in Fig. 7 for three different mean particle diameters of the niacin dust.

From the $v(x = d, t)$ profile, the VPR value, which is defined as the maximum value of $v(x = d, t)$, can be easily deduced for each dust and diameter considered.

From the VPR values, the K_{St} values at different particle diameters can be predicted using Equation (7). The predictions of the proposed model in terms of K_{St} values are summarized in the parity plot of Fig. 8, showing a general good agreement among

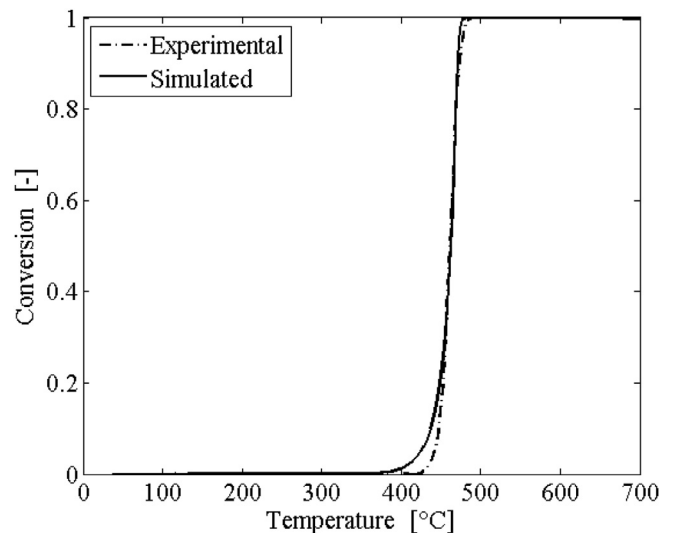


Fig. 6. Experimental and fitted conversion vs. temperature data for polyethylene. TG measurements carried out at 10 °C/min heating rate.

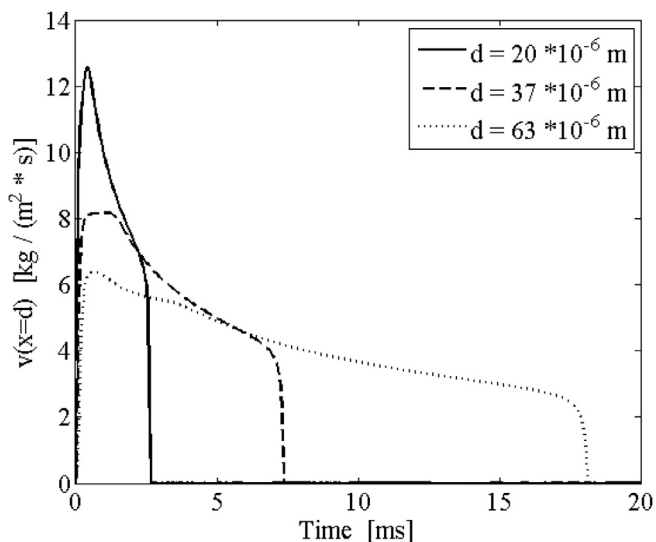


Fig. 7. $v(x=d)$ vs. time trends for different mean particle diameters of niacin dust.

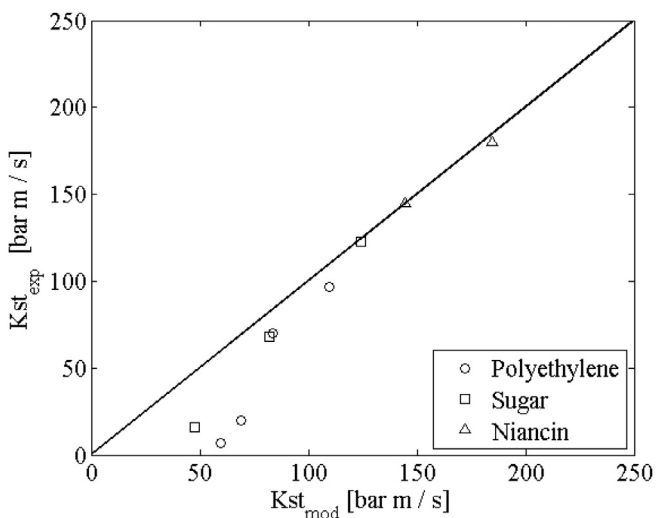


Fig. 8. Model predictions results vs Experimental data.

experimental data and model predictions for the investigated dusts.

The largest discrepancies have been found for the lowest K_{St} values (under 50 [bar m/s]), occurring for dust mean diameter above 150 μm : in correspondence of them, the model always over predicts the experimental data. However, such a conservative (from a safety point of view) behavior of the model is not a real problem because it is confined to very low K_{St} values. A possible explanation of this model behavior is related to the not fully compliance of assumption 2.

4. Conclusions

In this paper, a general methodology to predict the deflagration index K_{St} value for organic dusts as a function of their mean particle diameter has been presented and validated by comparison with experimental K_{St} values of three different organic dusts: polyethylene, sugar and niacin. Based on a single experimental datum, the K_{St} value for a reference dust mean diameter, the proposed methodology is able to foresee the strong reduction of the K_{St} value

when the dust mean diameter increases. Once further validated, this approach could possibly reduce the resources required for a complete hazard assessment when a large number of different dust mean diameter values are present in a production facility.

References

- Abbasi, T., Abbasi, S.A., 2007. Dust explosions-Cases, causes, consequences, and control. *J. Hazard. Mater.* 140, 7–44.
- Agreda, A.G., 2007. Study of Hybrid Mixture Explosions. PhD Thesis. American Society for Testing and Materials International, 2012. Standard Test Method for Explosibility of Dust Clouds, ASTM-e1226.
- Anderson, G.L., Higbie, H., Stegeman, G., 1950. The heat capacity of sucrose from 25 to 90. *J. Am. Chem. Soc.* 72 (8), 3798–3799.
- Ascher, U.M., Petzold, R.L., 1998. Computer Methods for Ordinary Differential Equations and Differential-algebraic Equations. SIAM.
- Cashdollar, K.L., Hertzberg, M., Zlochower, I.A., 1989. Effect of volatility on dust flammability limits for coals, gilsonite, and polyethylene. In: Proceedings of the 22nd Symposium (International) on Combustion, vol. 22, pp. 1757–1765 (1). Casson
- Moreno, V., Cozzani, V., 2015. Major accident hazard in bioenergy production. *J. Loss Prev. Process Industries* 35, 135–144.
- CBS website, «www.csb.gov». (Accessed 12 January 2017).
- Çengel, Y.A., 2008. Introduction to Thermodynamics and Heat Transfer, second ed. McGraw-Hill.
- CHETAH, 2009. Software 9.0.
- Contat-Rodrigo, L., Ribes-Greus, A., Imrie, C.T., 2002. Thermal analysis of high-density polyethylene and low-density polyethylene with enhanced biodegradability. *J. Appl. Polym. Sci.* 86 (3), 764–772.
- Dahoe, A.E., Cant, R.S., Pegg, R.S., Scarlett, B., 2001. On the transient flow in the 20-Litre explosion sphere. *J. Loss Prev. Process Industries* 14 (6), 475–487.
- Dahoe, A.E., Cant, R.S., Scarlett, B., 2002. On the decay of turbulence in the 20-liter explosion sphere. *Flow, Turbul. Combust.* 67 (3), 159–184.
- Di Benedetto, A., Russo, P., 2007. Thermo-kinetic modelling of dust explosions. *J. Loss Prev. Process Industries* 20, 303–309.
- Di Benedetto, A., Russo, P., Amyotte, P., Marchand, N., 2010. Modelling the effect of particle size on dust explosions. *Chem. Eng. Sci.* 65 (2), 772–779.
- Di Blasi, C., 1997. Linear pyrolysis of cellulosic and plastic waste. *J. Anal. Appl. Pyrolysis* 40–41, 463–479.
- DUST_EXPLOSION_RESEARCH website, «http://www.mydustexplosionresearch.com/explosion-incidents/». (Accessed 12 January 2017).
- Eckhoff, R.K., 2003. Dust Explosions in the Process Industries. Gulf Professional Publishing.
- Eckhoff, R.K., 2009. Understanding dust explosions. The role of powder science and technology. *J. Loss Prev. Process Industries* 22 (1), 105–116.
- Fornberg, B., 1988. Generation of finite difference formulas on arbitrarily spaced grids. *Math. Comput.* 51 (184), 699–706.
- Fornberg, B., 1998. Calculation of weights in finite difference formulas. *SIAM Rev.* 40 (3), 685–691.
- Fumagalli, A., Derudi, M., Rota, R., Copelli, S., 2016. Estimation of the deflagration index K_{St} for dust explosions: a review. *J. Loss Prev. Process Industries* 44 (1), 311–322.
- GESTIS-DUST-EX website, «http://staubex.ifa.dguv.de/?lang=e». (Accessed 26 October 2016).
- Glassman, I., Yetter, R.A., 2008. Combustion. Elsevier.
- Halford, J.O., 1957. Standard heat capacities of gaseous methanol, ethanol, methane and ethane at 279 K by thermal conductivity. *J. Phys. Chem.* 61, 1536–1539.
- Hertzberg, M., Zlochower, I.A., Cashdollar, K.L., 1988. Volatility model for coal dust flame propagation and extinguishment. In: Proceedings of the 21st Symposium (International) on Combustion, vol. 21, pp. 325–333 (1).
- Ilchmann, A., Reis, T., 2014. Surveys in Differential-algebraic Equations II. Springer, pp. 104–105.
- International Chemical Safety Card (ICS) 1507, 2003. Sucrose. International Programme on Chemical Safety, Geneva.
- Maccarthy, D.A., Fabre, N., 1989. Thermal conductivity of sucrose. Chapter of Food Properties and Computer-aided Engineering of Food Processing Systems, pp. 105–111. Volume 168 of the series NATO ASI Series.
- Maestre-Valero, J.F., Martínez-Alvarez, V., Baille, A., Martín-Gorri, B., Gallego-Elvira, B., 2011. Comparative analysis of two polyethylene foil materials for dew harvesting in a semi-arid climate. *J. Hydrology* 410 (1–2), 84–91.
- Mohos, F., 2010. Confectionery and Chocolate Engineering: Principles and Applications. Wiley-Blackwell.
- National Fire Protection Association, 2013. Standard on Explosion Protection by Deflagration Venting, NFPA 68.
- National Fire Protection Association website «http://www.nfpa.org/newsandpublications/nfpa-journal/2015/march-april-2015/features/dust». (Accessed 10 October 2015).
- Piergiorganni, L., Limbo, S., 2010. Food packaging: Materiali, tecnologie e soluzioni. Spinger-Verlag.
- Pu, Y.K., Jarosinski, J., Johnson, V.G., Kauffman, C.W., 1990. In: Turbulence Effects on Dust Explosions in the 20-l Spherical Vessel. 23rd Symposium (International) on Combustion. The Combustion Institute, Pittsburgh, pp. 843–849. Rabinovitch, B., 1965. Regression rate and the kinetics of polymer degradation. In: Proceedings of 10th International Symposium on Combustion. The Combustion

- Institute, Pittsburgh, pp. 1395–1397.
- Reyes, O.J., Patel, S.J., Mannan, M.S., 2011. Quantitative structure property relationship studies for predicting dust explosibility characteristics (K_{st} , P_{max}) of organic chemical dusts. *Industrial Eng. Chem. Res.* 50 (4), 2373–2379.
- Schiesser, W.E., 1991. *The Numerical Method of Lines*. Academic Press.
- Siwek, R., 1977. 20-L Laborapparatur für die Bestimmung der Explosionskenngrößen brennbarer Stäube. Thesis. HTL Winterthur, Switzerland.
- Sobrinho, J.A., Jiménez-Muñoz, J.C., Labed-Nachbrand, J., Nerry, F., 2002. Surface emissivity retrieval from digital airborne imaging spectrometer data. *J. Geophys. Res. Atmos.* 107 (23).
- Staggs, J.E.J., 2000. Simple model of polymer pyrolysis including transport of volatiles. *Fire Saf. J.* 34 (1), 69–80.
- Vande Wouwer, A., Saucez, P., Vilas Fernández, C., 2014. Simulation of ODE/PDE Models with MATLAB®, OCTAVE and SCILAB Scientific and Engineering Applications. SPRINGER.
- Wang, C., Dou, B., Song, Y., Chen, H., Yang, M., Xu, Y., 2014. Kinetic study on non-isothermal pyrolysis of sucrose biomass. *Energy Fuels* 28 (6), 3793–3801.
- Wichman, I.S., 1986. A model describing the steady-state gasification of bubble-forming thermoplastics in response to an incident heat flux. *Combust. Flame* 63 (1–2), 217–229.
- Zhen, G., Leuckel, W., 1996. Determination of dust-dispersion-induced turbulence and its influence on dust explosions. *Combust. Sci. Technol.* 113–114, 629–639.